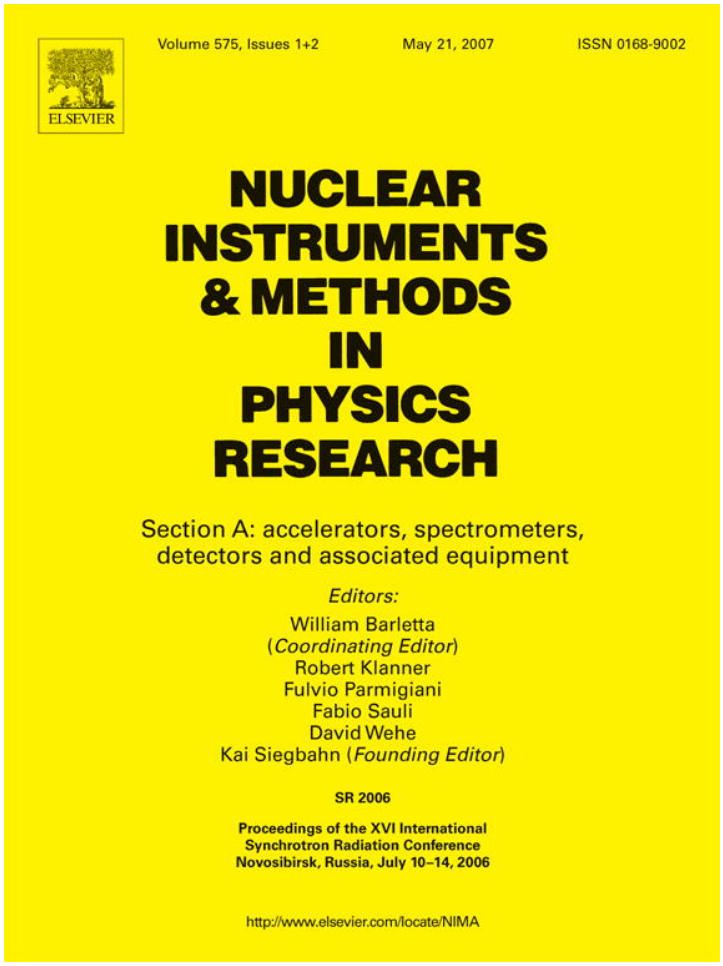

Available online at www.sciencedirect.com
ScienceDirect
Nuclear Instruments and Methods in Physics Research A 575 (2007) 121–125
NUCLEAR INSTRUMENTS & METHODS IN PHYSICS RESEARCH Section A
www.elsevier.com/locate/nima

Synchrotron diagnostics of shock-wave compression of aerogel

L.A. Merzhievsky[a,*], L.A. Lukianchikov[a], E.R. Pruuel[a], K.A. Ten[a], V.M. Titov[a], B.P. Tolochko[b], E.V. Evdokov[b], I.L. Zhogin[b], M.A. Sheromov[c]

[a]*Lavrentiev Institute of Hydrodynamics SB RAS, Novosibirsk, Russia*
[b]*Institute of Solid State and Mechanochemistry SB RAS, Novosibirsk, Russia*
[c]*Budker Institute of Nuclear Physics SB RAS, Novosibirsk, Russia*

Available online 13 January 2007

Abstract

This work describes the procedure for investigation into dynamics of shock-wave compression of aerogel with the help of synchrotron radiation (SR). The aim of the experiments was to measure intensity both of transmitted radiation, giving information on substance density variation, and of radiation scattered through small angles (small-angle X-ray scattering (SAXS)), that can be used for reconstruction of pore evolution. The studies have shown that the SAXS signal vanishes while the shock wave is passing, i.e. the pores practically get shut. The porous structure of the substance recovers after the shock wave has passed, however, with a different pore size-grade distribution.

PACS: 07.85.F; 47.40.N; 78.70.C

Keywords: Explosives; Synchrotron radiation; SAXS; Shock wave; Density distribution

1. Introduction

Aerogels are highly porous materials, ultimately low density and large amount of small-size pores being their main particularities. Besides, these materials are specific physical objects macroscopic clusters of rigidly-connected particles with a typical size of a few nanometers. The rigid frame is a small part of aerogel volume, i.e. almost all its volume (up to 98–99% and more) falls at pores. The very first aerogel was obtained by Kistler [1] from silica in 1930–1931. Later on they managed to obtain aerogels from aluminum, tungsten, iron, tin, and carbon oxides and a number of organic compounds and substances. According to the existing conceptions, there are no principal restrictions on obtaining aerogels from practically any material.

Owing to these structural particularities, aerogels have unique physical features. One of the most important properties is their low heat conductivity combined with relatively high transparency [2]. Sound speed in aerogels is even lower than that in gases. The first information on the sizes of structural elements of aerogels was obtained using the Rayleigh light scattering. Literature present results of study of pore size-grade distribution using mercury porosimetry, thermal porosimetry, and methods basing on adsorption and desorption of various substances, e.g. nitrogen. These methods can disturb the aerogel structure very much, which casts some doubt on the results and requires their thorough analysis. Photographing samples with electron microscope in transmitted and reflected rays also has some disadvantages since, as research shows, electron beam influence can lead to enlargement of structural elements of aerogels. The most reliable method to analyze structure of aerogels is the small-angle scattering of X-ray or neutrons. A simplest model of aerogel [3] can be created from spherical "primary" particles of a radius $r_0 \leqslant 1$ nm united in "secondary", also spherical particles, forming chains in which particles become bound when they touch each other. Namely, these chains make the high-porous structure of aerogel. In the size range $r_0 \leqslant r \leqslant R_0$ (R_0 is the maximal pore size) aerogel is a fractal cluster and at $r \gg R_0$ it is considered as a homogeneous body.

*Corresponding author. Tel.: +7 383 333 18 99.
E-mail address: merzh@hydro.nsc.ru (L.A. Merzhievsky).

0168-9002/$ - see front matter © 2007 Elsevier B.V. All rights reserved.
doi:10.1016/j.nima.2007.01.040

As aerogel is subjected to high-intensity external impact in some of its possible applications, it would be of interest to study aerogel properties and behavior at dynamical and shock-wave loading. In this connection, we should mention several works concerning construction of shock adiabats and equations of state for a silicon aerogel [4–8].

This work takes the advantages of synchrotron radiation (SR) in order to study behavior of an aerogel on the base of silicon dioxide (SiO_2) at shock-wave loading. SR applicability in the study of explosion and shock-wave processes was shown in Refs. [9–11].

2. Structural and mechanical characteristics

Fig. 1 gives a general picture of the structure of the SiO_2 aerogel under study. It presents photos of micro-samples of various densities, made with a transmission electron microscope (TEM). Density of the material in Fig. 1 is $0.15\,g/cm^3$. The size distribution of pores for sample 1, obtained by the nitrogen adsorption method, is presented in Fig. 2 (the number of pores in relative units as a function of the size). The maximum of distribution falls at pores with a diameter of ≈ 25 nm and the sizes of most pores are within the range of 20–40 nm. If the density decreases, the maximum distribution moves towards larger pores and the distribution itself becomes wider because of the presence of larger pores (as large as 70–80 nm).

Elastic properties of the aerogel under study loading were determined in uniaxial compression experiments. A diagram of deformation of a sample with an initial density of $0.25\,g/cm^3$ is presented in Fig. 3 (the dots are the experimental data). It can be seen that the relationship between the stress and deformation is linear practically till

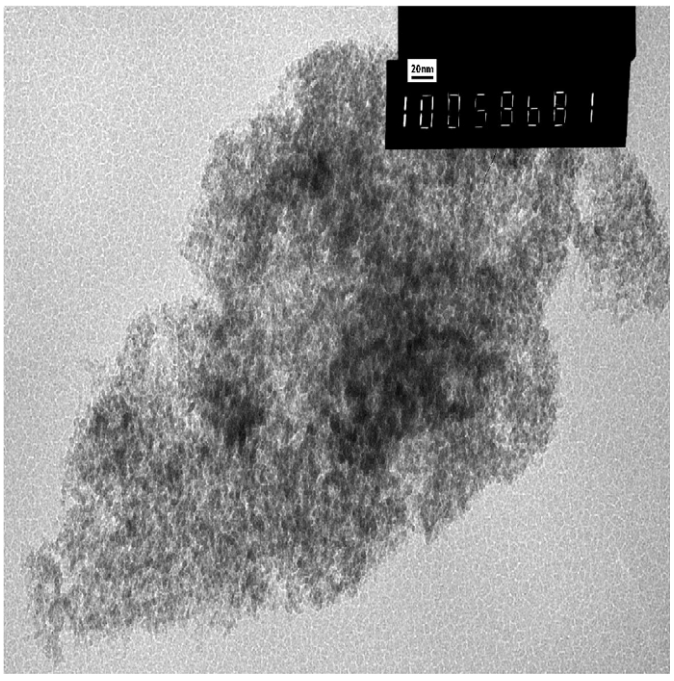

Fig. 1. The structure of aerogel.

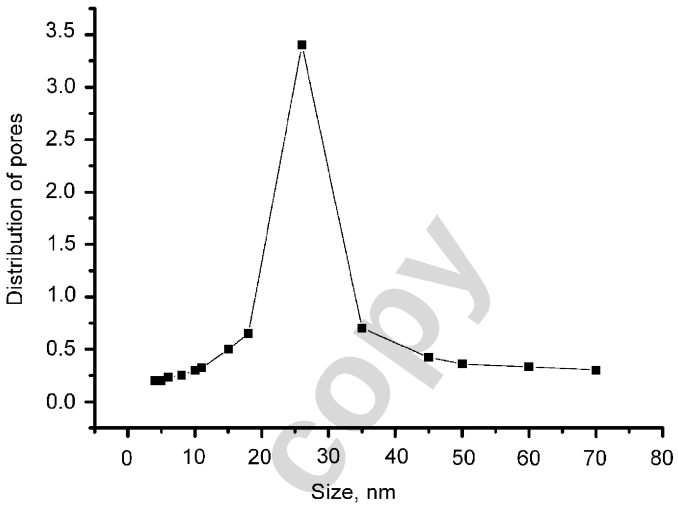

Fig. 2. Distribution of pores for aerogel.

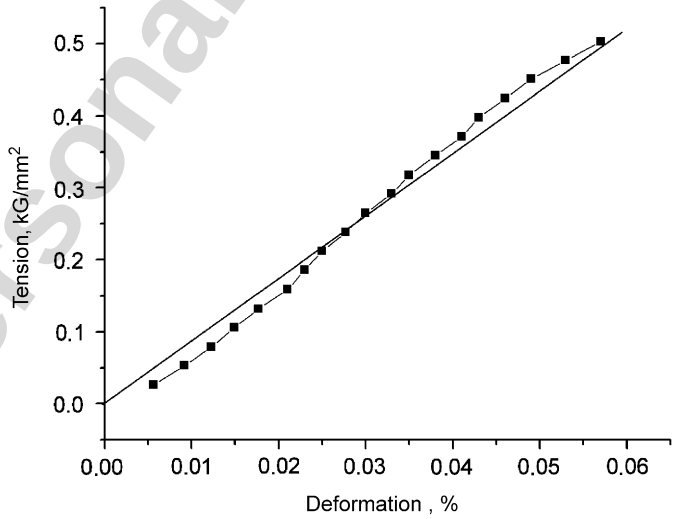

Fig. 3. A diagram of deformation of a sample with an initial density of $0.25\,g/cm^3$.

the moment of destruction (the last dot corresponds to it). The Young modulus calculated with the data presented is $\approx 0.5\,kg/mm^2$; the limiting deformation is ~ 0.057.

3. Experimental set-ups

A experimental set-ups to study detonation and shock-wave processes is described in detail in Refs. [9,10]. In this work, cylindrical aerogel samples of diameters and lengths of 10, 15 and 20 mm were subjected to loading, which was realized in two ways. In the first case, the plane shock wave was excited on one of the ends of the sample, via blowing up an explosive charge (also cylindrical) contacting with the sample, either directly or through an insertion. Curvature of the front of the loading detonation wave was monitored beforehand with the use of high-speed photography. According to the photography results, the front could be considered to be flat with an accuracy of

~2%, for all explosive charges applied. In the second variant, the shock wave in the sample was excited by a impact of a plate accelerated by explosive detonation products through the air gap. Direct SR measurement showed that the plate was remaining practically flat during all the time of the experiment.

Parameters of the shock-compressed aerogel were measured with the SR beam. The experimental set-ups was placed horizontally along the plane of the formed SR beam 0.4 mm high and ≈18 mm wide. The shock wave in the aerogel was in the SR beam zone for 3–4 μs and we managed to take 6–8 photos (with an exposure of 1 ns) of radiation transmitted and scattered over small angles along the sample axis. The time interval between the frames was ≈ 500 ns. The radiation was registered by the detector DIMEX [9], that was also placed along the set-ups axis, in a distance of 770 mm from it. The registration channel was 1 mm high and 0.1 mm long, along the charge axis. The total number of channels was 256 (26.5 mm). The detector got activated when the contact sensor in a distance of 15 mm beyond the beam arrival area was closed. Variation of intensity of the beam transmitted through the sample gives information on density distribution in the measurement area, and intensity of the beam part diverting over small angles (small-angle X-ray scattering (SAXS)) allows calculating the sizes and number of structural elements of the aerogel (for details see Ref. [9]).

4. Measurements in the transmitted ray

Fig. 4 (Loading with an explosive charge, the resulting intensity referred to the initial one after the sample in the non-loaded state, or relative intensity) gives the picture of transmitted radiation intensity variation as the shock wave is moves over the aerogel. Even together with instrumental smearing of signal (a "point signal" excites three registration channels), it can be seen that the loading pulse front is notably smeared owing to the high porosity of the material. The shock-wave speed is constant and equals ~2.4 km/s.

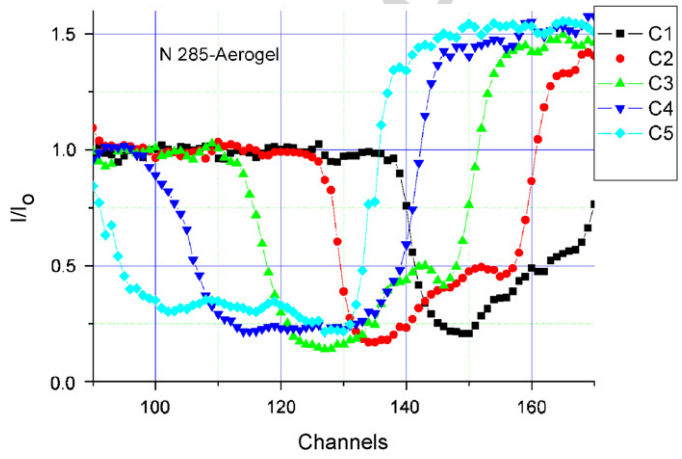

Fig. 4. Shock compression of aerogel by explosive. Time between frames −0.5 μS.

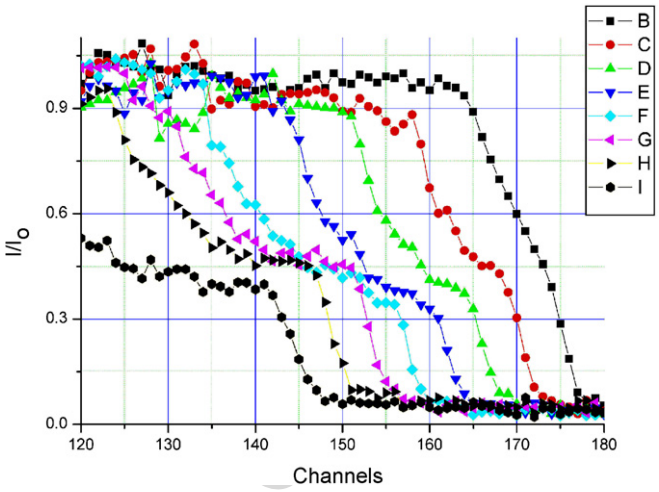

Fig. 5. Shock compression of aerogel by piston. Time between frames −0.5 μS.

Similar data for the case of shock loading of the piston are presented in Fig. 5. In this case, besides the velocity of shock wave, its mass velocity beyond the front is measured, which equals the velocity the piston is flying with. The data obtained can be compared with the shock adiabats [4–8] and can be used as a base for shock adiabats for the aerogels of different initial densities.

5. SAXS intensity measurement

In each experiment of this series, we registered simultaneously SAXS spatial distribution and transmitted radiation distribution ($\theta \approx 0$). It allowed us to correlate the observed SAXS distribution with the moment of shock wave arrival and subsequent unloading in the observation zone. An example of the results is shown in Fig. 6 (the shock-wave speed is 3.4 km/s). Fig. 6(a) presents the results for an initial sample in the non-loaded state.

Large structural non-uniformity of the material, in which small high-density particles of SiO_2 alternate with big-size pores, caused intense small angle scattering of the probing beam. Guinier processing of SAXS intensity distribution dependencies on the scattering angle after smoothing them by standard methods makes it possible to construct a size distribution function for particles composing the aerogel. SAXS distributions in the non-compressed (points C) and compressed (points D) material are compared in Fig. 6(a). According to the data, there is practically no SAXS in the shock-compressed material, which evidences its relative uniformity (absence of density fluctuations) in the compressed state. SAXS distributions in the initial state (points C) and after the shock-wave transmission and subsequent unloading (points G) are compared in Fig. 6(b). The pore structure of the material has recovered after the unloading. However, the distribution of sizes of scattering particles has changed as evidenced by the difference in the curves corresponding to points C and G. According to data on transmitted beam

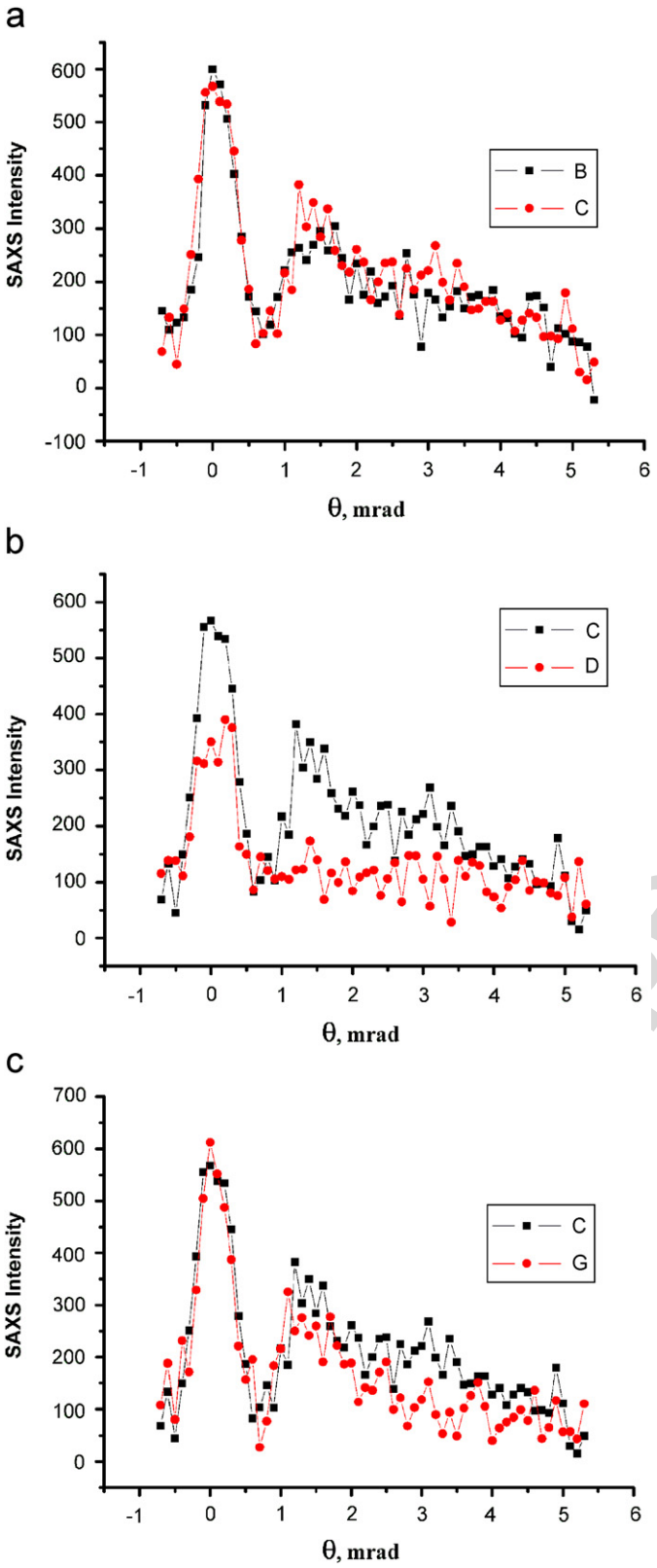

Fig. 6. (a) C—Initial SAXS distributions in aerogel, D—at shock compression. (b) C—Initial SAXS distributions in aerogel, G—after shock compression.

intensity, density of the material after the unloading is close to the initial one.

Different data on aerogel state after unloading were obtained at loading with shock waves of lower intensities. In this case, SAXS distributions in the initial and unloaded states are practically the same, which is a result of complete recovery of aerogel structure after the shock-wave transmission and subsequent unloading. According to the obtained data, the critical amplitude of shock wave, starting from which the aerogel structure changes in quality at shock-wave loading, corresponds to a shock-wave velocity of ~2.8 km/s.

6. Discussion of results

Shock adiabats of aerogels of different initial densities are constructed in works [4–8] in the form of linear relationship between the shock wave speed D and mass speed beyond its front U. The experimental data for aerogels with density of 0.008–0.36 g/cm^3 are generalized in a unified shock adiabat, in the form of linear and quadratic relationship of D with U in Refs. [7,8], correspondingly. These shock adiabats describe the results of our experiments with admissible accuracy.

Methods applying nitrogen adsorption, electron microscopy and SR were used to study mesostructure of aerogel in the initial state. It was revealed that the average pore size (the maximum of the distribution function) is approximately one order higher than the average size of particles composing aerogel. SR methods allowed us to reveal presence of a meso-structure transition in aerogel when the critical parameters of shock wave are achieved. The essence of the transition is that the size of aerogel particles that dissipate the radiation over small (Fig. 7). angles changes at the speed $D > D_K$ (the approximate value $D_K \approx 2.8$ km/s is to be defined more accurately). This statement is illustrated in Fig. 7, where points B show distribution of particle sizes

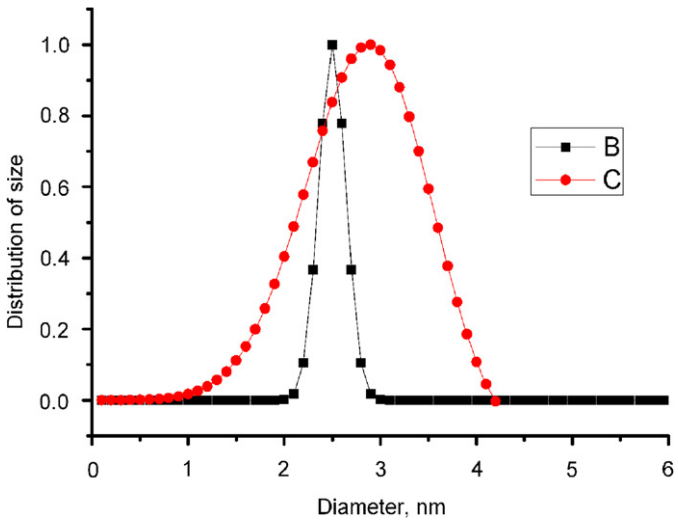

Fig. 7. Distribution of particle sizes after shock-wave loading: B—for $D < D_K$ and C—for $D > D_K$.

after shock-wave loading at $D<D_{K,}$ and points C show that for $D>D_K$. The distribution in case B is rather narrow and practically coincides with the distribution of aerogel particles size in the initial state (before the loading). The C distribution demonstrates a significantly broader range of particle size, both smaller and larger particles increasing in number. The average aerogel density after unloading remains close to the initial one in both cases (naturally, before the aerogel begins dispersing).

Acknowledgments

The work has been carried out with the support of RFBR Grants Nos. 06-02-17335, 05-03-32752, SB RAS Integration project No. 23 and RAS Presidium Program, state contract No. 4/06.

References

[1] S.S. Kistler, Nature 127 (3221) (1931) 741.
[2] B.M. Smirnov, Aerogels, Uspekhi Fizicheskikh Nauk 152 (1) (1987) 133 (in Russian).
[3] I. Frike, V. Mire Nauki (7) (1988) 50 (in Russian).
[4] R. Rabie, J.J. Dick, Equation of state and crushing dynamics of low-density silica aerogels, Shock Compr. Condens. Matter. (1991) 87–90.
[5] N.C. Holmes, E.F. See, Shock compression of low-density microcellular materials, Shock Compr. Condens. Matter. (1991) 91–94.
[6] V.E. Fortov, A.S. Filimonov, V.K. Gryaznov, D.N. Nikolaev, V.Ya. Ternovoi, Mod. Phys. Lett. A 18 (26) (2003) 1835.
[7] V.C. Vildanov, M.M. Gorshkov, V.M. Slobodenjukov, E.H. Rushkovan, Shock compression of low initial density quartz at pressures up to 100 GPa, Shock Compr. Condens. Matter (1995)121–124.
[8] M.V. Zhernokletov, T.S. Lebedeva, A.B. Medvedev, M.A. Mochalov, A.N. Shuykin, V.E. Fortov, Thermodynamic parameters and equation of state of low-density SiO_2 aerogel, Shock Compr. Condens. Matter (2001) 763–766.
[9] A.N. Aleshaev, P.I. Zubkov, G.N. Kulipanov, L.A. Lukianchikov, N.Z. Lyakhov, S.I. Mishnev, K.A. Ten, V.M. Titov, B.P. Tolochko, M.G. Fedotov, M.A. Sheromov, Combus. Explos. Shock Waves 37 (5) (2001) 104.
[10] P.I. Zubkov, G.N. Kulipanov, L.A. Lukianchikov, L.A. Merzhievsky, K.A. Ten, V.M. Titov, B.P. Tolochko, M.G. Fedotov, M.R. Sharafutdinov, M.A. Sheromov, Explos. Shock Waves 39 (2) (2003) 137.
[11] L.A. Merzhievsky, P.I. Zubkov, L.A. Lukianchikov, K.A. Ten, V.M. Titov, G.N. Kulipanov, M.G. Fedotov, M.A. Sheromov, B.P. Tolochko, M.R. Sharafutdinov, Issues Atom. Sci. Eng. Ser. Mater. Sci. New Mater. 2 (63) (2004) 383.